Vision Research, Vol. 18, pp. 815–825

0042-6989/78/0701-0815$02.00/0

GRATING SUMMATION IN FOVEA AND PERIPHERY[1]

NORMA GRAHAM*, J. G. ROBSON† and JACOB NACHMIAS‡

*Department of Psychology, Columbia University, New York, NY 10027, U.S.A.;
†Physiological Laboratory, Cambridge University, Cambridge, England; and
‡Department of Psychology, University of Pennsylvania, Philadelphia, PA 19174, U.S.A.

(*Received* 10 *April* 1977; *in revised form* 15 *September* 1977)

Abstract—Results from previous studies measuring the detectability of sinusoidal gratings have been interpreted by models postulating several sizes of receptive fields. It has not been clear, however, whether or not these several sizes coexist at a single position in the visual field. Perhaps there is only one size centered at each position, but the size varies as a function of eccentricity.

In this study, the detectability of compound gratings containing two sinusoidal components was compared to that of each component alone. Measurements were made in the fovea and 7.5° into the periphery. Stimuli were localized in a small region of the visual field and sharp spatial and temporal transients eliminated by weighting grating contrast with Gaussian functions of space and time. To reduce possible effects of expectation, bias and frequency uncertainty, a temporal, forced-choice, interlaced staircase procedure was used. The results are consistent with models postulating several sizes of receptive fields at each position in the visual field but not with models postulating only one size at each position, even when the size varies as a function of eccentricity to account for the differences in spatial interaction characteristic of different parts of the visual field.

INTRODUCTION

Sine-wave summation experiments have provided some of the strongest support for the notion of independent channels in the human visual system, each sensitive to a different range of spatial frequency. These experiments have shown that a compound grating containing two or three sinusoidal components of far-apart frequencies is only slightly more detectable than its most detectable component; further, the detectability of such a compound grating does not depend on the relative phase of its components (Campbell and Robson, 1964, 1968; Sachs, Nachmias and Robson, 1971; Graham and Nachmias, 1971; Lange, Sigel and Stecher, 1973; Kulikowski and King-Smith, 1973; Pantle, 1973; Quick and Reichert, 1975; Mostafavi and Sakrison, 1976; Robson and Graham in Graham, 1978).

All the experiments, however, have had features which preclude rigorous analysis. In the study reported here, we attempted in the following ways to provide more unambiguously interpretable results. First, a two-alternative forced-choice staircase procedure was used to minimize effects of observer expectation and bias. Then the different patterns were randomly intermixed so that the observer could not change his strategy for different patterns, i.e. there was frequency uncertainty.

Further, we used patches of grating in which the contrast was weighted by a Gaussian function of space and time. Thus, all spatial and temporal transitions were gradual. These gradual transitions eliminate the complications introduced by sharp edges. Spatial edges, in particular, complicate theoretical interpretation because of the extra spatial frequencies introduced by edges and the possibility of special effects of edges *per se*.

Another complication in interpreting previous experiments resulted from the well-known variation in the characteristics of spatial interaction at different positions in the visual field (e.g. Aulhorn and Harms, 1972; Green, 1970; Hines, 1976). Many lines of evidence suggest that the smallest receptive fields are located nearest the foveal center while larger receptive fields are located more peripherally. This non-uniformity makes it difficult to interpret unambiguously the results of previous sine-wave summation experiments. It could be argued that, while the high spatial frequency component in complex gratings is detected near the foveal center, the low frequency component is detected in the periphery. It this were true, previous experiments would not have conclusively shown whether or not several channels sensitive to different ranges of spatial frequency actually co-exist in the same region of the visual field (van Doorn, Koenderink and Bouman, 1972; Limb and Rubinstein, 1977). In our experiments, use of the spatial Gaussian weighting function reduced the effect of spatial non-uniformity by effectively localizing the stimuli in a small region without introducing too many unwanted spatial frequencies.

The problem of non-uniformity of the visual field was further approached by studying sine-wave summation using stimuli presented peripherally as well as centrally. If the periphery is more uniform than the fovea, as has been supposed (e.g. Limb and Rubinstein, 1977), the low and high frequency components of a compound grating presented peripherally are more likely to be detected at exactly the same spatial location than are the components of a compound grating presented centrally. Then, if there is only one spatial-frequency channel at each spatial

[1] This work was supported in part by grants from the National Science Foundation (BMS 75-07658 to J.N. and BNS 76-18839 to N.G.). The main experiments were carried out at J.G.R.'s laboratory using equipment provided by the Medical Research Council. A subsidiary experiment reported in Table 1 was carried out at J.N.'s laboratory.

location, the components of a compound grating presented peripherally are more likely to be detected by the same spatial-frequency channel than are the components of a compound grating presented centrally. In this case, the compound grating presented peripherally would be much more detectable than the compound grating presented centrally.

METHODS

Stimulus

Each stimulus was a small patch of vertically oriented grating—containing components with frequencies 2 c/deg, 6 c/deg, or both—centered either at the fixation point or 7.5° to the right. The stimulus did not have sharp edges. Instead, the contrast of the grating was weighted by a Gaussian function of both horizontal (x) and vertical (y) spatial position. This Gaussian function had a space constant of 0.75° of visual angle; that is, the contrast of the pattern fell to 1/e (about 37%) of its peak value at 0.75° from its center. Furthermore, the stimulus was turned on and off gradually. The temporal profile of contrast was a Gaussian function of time with a time constant of 100 msec; that is, the contrast of the grating was above 37% of its peak value for 200 msec. Formally, the luminance $L(x, y, t)$ at each point (in space and time) of the stimulus patch can be written in terms of a weighting function $w(x, y, t)$ and the sinusoidal components $g(x)$. The weighting function can be separated into $w_1(x)w_2(y)w_3(t)$. Let L_0 = the mean luminance (400 cd/m^2), m_2 = the contrast in the 2 c/deg component, m_6 = the contrast in the 6 c/deg component, the θ = the phase angle between the components. Then

$$L(x, y, t) = [w(x, y, t) \cdot g(x) + 1] \cdot L_0 \quad (1)$$

where

$$w(x, y, t) = w_1(x) \cdot w_2(y) \cdot w_3(t) = \exp\left(-\frac{(x^2 + y^2)}{(0.75\,\text{deg})^2}\right) \cdot \exp\left(\frac{t^2}{(0.1\,\text{sec})^2}\right) \quad (2)$$

and

$$g(x) = m_2 \cdot \sin(2\pi 2x) + m_6 \cdot \sin(2\pi 6x + \theta). \quad (3)$$

The point where x and y are zero is the midpoint of the stimulus (located either at foveal center or 7.5° to the right). The instant when t is zero is the temporal midpoint.

Figure 1 shows the luminance profile of these stimuli as a function of horizontal position—that is, L as a function of x, $L(x, 0, 0)$. The figure includes a 2 c/deg stimulus, a 6 c/deg stimulus, and two combinations of 2 and 6 c/deg for which there is equal contrast in the 2 c/deg and the 6 c/deg components. In the peaks-add combination (right), $\theta = 180°$. In the peaks-subtract combination (left), $\theta = 0°$.

Details of the stimulus. The horizontal luminance profiles of these stimuli are not, of course, pure sinusoids. Since they are not infinite in spatial extent, they contain a range of frequencies. The range, however, is quite narrow. The amplitude of the Fourier transform is above 37% of its peak for a range of only $8/3\,\pi$ c/deg (that is, from 1.58 to 2.42 c/deg in the case of the nominal 2 c/deg stimulus and from 5.58 to 6.42 c/deg in the case of the nominal 6 c/deg stimulus).

The stimuli were produced by modulating the cathode current of a cathode-ray tube whose beam was electromagnetically deflected by a 100 Hz sawtooth and a 150 kHz triangular wave to generate a raster display. A feedback circuit was used to ensure that the cathode current (and hence, over a very wide range, the screen luminance) was proportional to the applied modulating voltage. This modulating voltage was produced as the product of two signals. The signal determining $g(x) \cdot w_1(x) \cdot w_3(t)$ was generated by converting the digital output of a computer (clocked at 80 kHz) to an analogue signal, low-pass filtering it (0–45 kHz), and attenuating it under computer control. The resulting analogue signal was multiplied by a Gaussian pulse synchronized with the line-deflection waveform to introduce the variation of contrast in the vertical direction, $w_2(y)$.

The exposed area of the CRT was quite large—29 cm wide by 20 cm high. This gave a display of 14.5° by 10° at the viewing distance used (115 cm). The foveal patches were centered 3.5° from the left edge of the screen, the peripheral patches 3.5° from the right edge. The CRT screen was seen through a rectangular hole in a large screen (61 × 61 cm) illuminated so as to approximate the CRT in luminance and hue. The mean luminance was constant throughout the experiment at 400 cd/m^2. The CRT

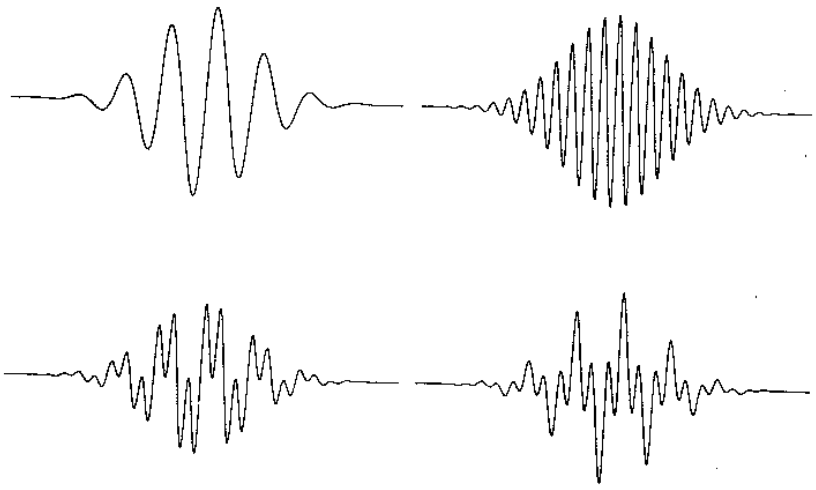

Fig. 1. The horizontal luminance profiles of patterns used in this study. Upper left: patch containing only the 2 c/deg component. Upper right: patch containing only the 6 c/deg component. Lower left: patch containing both components at equal amplitude in peaks-subtract phase. Lower right: patch containing both components at equal amplitude in peaks-add phase. The sum of the amplitudes in the two components is the same in all four patterns.

phosphor was P31 and appeared to be desaturated green.

The stimuli were viewed binocularly with natural pupils. When the stimuli were peripheral, the subject fixated directly a small dot on the face of the CRT. When the stimuli were foveal, the subject fixated halfway between two small vertical lines positioned slightly above and below the grating patch.

Psychophysical procedure

Thresholds were determined by a two-temporal alternative forced-choice interlaced staircase procedure. The word "pattern" will refer to a particular ratio of contrasts in the 2 and 6 c/deg components at a particular phase. Thus, to determine the threshold contrast for a particular pattern, the contrasts in both the 2 and 6 c/deg components were changed while keeping their ratio constant.

Trials of several patterns (ranging from 4 to 10 in different sessions) were randomly intermixed under computer control. Thus, the subject never knew whether the next stimulus would be 2 c/deg alone, 6 c/deg alone, or one of several ratios of 2 and 6 c/deg in either of two different phases. In any one session, however, unless otherwise noted, the patterns were all presented in the fovea or all in the periphery.

Details of a trial. The observer started each trial by pushing a button. Then followed the two stimulus intervals, each 600 msec long (although the stimulus was above 37% of its peak for only the middle 200 msec), separated by about 300 msec. The stimulus intervals were indicated by tones. At the end of the trial, the observer pushed one of two buttons to indicate which interval he thought had contained the stimulus. Tone feedback indicated which interval had actually contained the stimulus.

Details of the staircase procedure. Although the thresholds for several different patterns were in fact always determined concurrently, the staircase procedure is most easily understood if it is described at first as though only one pattern were involved. At the beginning of the staircase, the contrast of the pattern was haphazardly set to be about one-quarter to one-half of a log unit above the expected threshold. Four trials (comprising a step in the staircase) were then made at this contrast. The contrast was then changed by $+4$, $+3$, $+2$, $+1$ or -1 units, depending on whether the observer had made zero, one, two, three or four correct responses in the last four trials. Subsequently, after each further step of four trials, the contrast was changed according to the same rule. What constituted a unit of contrast change was determined by the number of times the staircase had reversed direction. After zero, one, two, three or four or more reverals, the unit of contrast change was 0.175, 0.1125, 0.625, or 0.05 log units, respectively. Then the threshold was computed as the mean of the contrast values (expressed on a logarithmic scale) of all steps following the fifth reversal.

In an actual experiment, where the staircases for several patterns were run concurrently, the four trials of each pattern required at a particular step were randomly intermixed. Otherwise, the staircases for the several different patterns were independent. A set of staircases continued until the staircase for every pattern had progressed for at least two steps past its fifth reversal. A set of staircases had, on average, 15 steps, and took 20–40 min to run. It provided, for each pattern involved in it, a threshold estimate that was calculated from the contrast values on the final, on average, 5.5 steps.

In order to determine what point on the psychometric function this staircase procedure estimates, the data from the staircases were reanalyzed in terms of the percentage correct at each contrast level. The computed threshold turned out to be that contrast giving approximately 90% correct.

Details of a session. Generally, both observers participated in any one session. They observed for alternate sets of staircases using the same patterns, and a session was usually continued until both observers had viewed 5 sets of staircases. Each set provided one estimate of threshold contrast for each pattern.

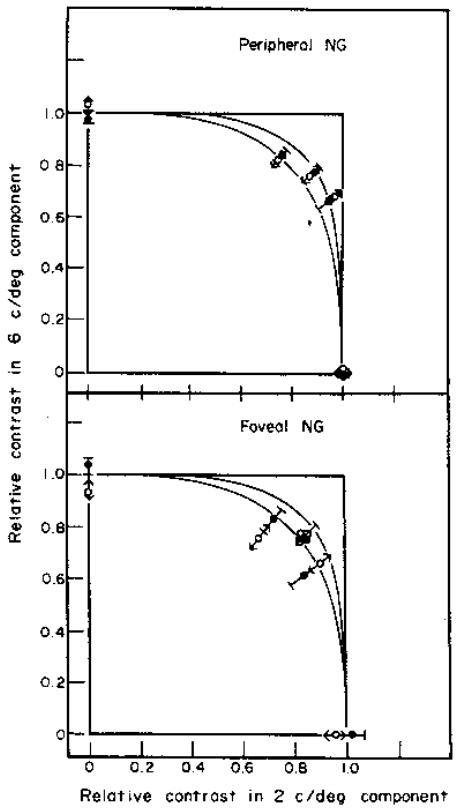

Fig. 2. Obtained thresholds for patterns containing 2 c/deg and/or 6 c/deg for observer NG. Horizontal axes give contrast in the 2 c/deg component of the pattern at threshold relative to the threshold contrast for 2 c/deg alone. Vertical axes give contrast in the 6 c/deg component relative to the threshold contrast for 6 c/deg alone. Results for the two positions (foveal on bottom, 7.5° peripheral on top) are shown. The thresholds for peaks-subtract and peaks-add patterns are given by solid and open symbols, respectively.

The solid curves are predictions from a model assuming multiple independent channels. They are the same as the curves marked 3 and 4 in Fig. 4.

Observers

The authors whose vision was normal when corrected (JGR and NG) were the observers in this experiment. Although they knew the purpose of the experiment, the two-alternative forced-choice procedure protected against the possible influence of their expectations.

RESULTS

At both the foveal and peripheral (7.5° to right) positions, several different ratios of contrast in the 2 and 6 c/deg components were used. For each ratio of contrast, both the peaks-add and peaks-subtract phases were used.

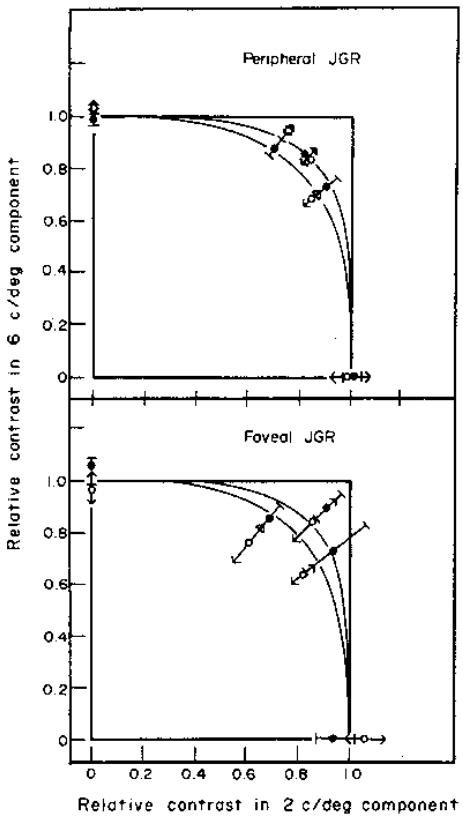

Fig. 3. Same as Fig. 2 except that the observer is JGR.

Figures 2 and 3 show the results of the two observers (NG in Fig. 2) for both positions of pattern (peripheral on top, foveal on bottom). Peaks-subtract and peaks-add patterns are represented by solid and open symbols, respectively. The contrast in the 6 c/deg component of the pattern at threshold is given on the vertical axis and that in the 2 c/deg component on the horizontal axis. The contrasts are given relative to the contrast thresholds for each component when presented by itself.

Briefly, very similar results were obtained for both retinal positions, both phases, and both observers. All the thresholds fall near the solid lines which, as will be explained further below, are the predictions from a model involving probability summation among multiple independent channels.

The threshold contrasts used in plotting Figs 2 and 3 were the averages of all the thresholds collected in individual blocks. (The averaging was carried out on the thresholds expressed on a logarithmic scale.) The threshold contrasts in Figs 2 and 3 are given relative to the best estimates of the contrast thresholds for 2 c/deg alone and for 6 c/deg alone. To calculate the horizontal coordinate of a point, for example, the actual contrast in the 2 c/deg component of the pattern at threshold was divided by the best estimate of the threshold contrast for 2 c/deg alone. The best estimate for the threshold of a single frequency was taken to be the average of all the thresholds from individual blocks for that frequency alone, whether the nominal phase was peaks-add or peaks-subtract (whether θ was 180° or 0° in Eqn 3). This averaging across phases is certainly appropriate for 2 c/deg (for which m_6 in Eqn 3 is zero) since the nominal phase makes no difference in the physical pattern. For 6 c/deg (m_2 equals zero in Eqn 3) nominal phase does make a difference in the pattern, equivalent to exchanging peaks and troughs, and it is conceivable that the true thresholds for the two phases might be different. There is no evidence for any consistent difference in thresholds, however, in Figs 2 and 3. Therefore, the disparity between the open and the closed symbols lying on either a vertical or horizontal axis can be taken as an indication of the variability inherent in the data. The values of the best estimates of threshold contrast for JGR and NG, respectively, were: 0.013 and 0.014 for 2 c/deg in the fovea; 0.041 and 0.044 for 2 c/deg in the periphery; 0.011 and 0.012 for 6 c/deg in the fovea; and 0.057 and 0.070 for 6 c/deg in the periphery.

Another indication of the variability is given in the figure by the error bars around each point, which represent plus and minus one standard error of the mean. Since the ratio of contrasts in any one pattern was kept constant, the error bars are along lines of constant ratio (lines through the origin). That the error bars are of different lengths should not be taken as evidence that some patterns in some conditions lead to more variability than others. The expected standard errors varied because the number of blocks (and therefore the numbers of values entering into the average) varied. The number of blocks ranged from 5 to 25 (depending on the exigencies of time and scheduling constraints) with, in general, more blocks for the simple gratings (points on the axes) and for the gratings in which the components were mixed as equally as possible (near the positive diagonal), and more blocks for the peripheral than for the foveal condition. Once this factor is taken into account, there are no reliable differences in the standard errors for different patterns or different conditions. The standard deviation of the population of values for any pattern is about 0.045 log units of contrast. The standard error for the average of a group of 5 values is thus about 0.02 log units, and for a group of 20 values about 0.01 log units.

Our results do not completely agree with those recently reported by Limb and Rubinstein (1977). They show (their Fig. 23) a small but significant phase effect for stimuli in the periphery. Further, comparison of their Fig. 23 with our Figs 2 and 3 shows that their complex gratings, particularly those in the peaks-subtract phase, were less detectable (relative to simple gratings) than were ours. It is hard to be certain of the explanation for these discrepancies. That their complex gratings were relatively less detectable than ours may be due to a frequency uncertainty effect (see below). There were also other differences in experimental conditions: they used uniform-amplitude patches of grating with 11° bars; their frequencies were 1 and 3 c/deg; their mean luminance was lower than ours; their observer viewed the display monocularly, ours binocularly.

Monocular viewing

To investigate the possibility that in our experiment, where the observers viewed the patterns binocularly, the two components of the pattern may have been detected by different eyes, we ran an additional experiment in which the observers viewed the patterns monocularly. The experimental conditions and procedures were like those described above except that the CRT had been rotated so that the gratings were horizontal and appeared 7.5° above the fixation point. Both observers used their right, dominant eyes, covering the left eyes with translucent paper that admitted some light but no detail. Four patterns were studied: 2 c/deg alone, 6 c/deg alone, and both together in each of two phases (with the contrast ratio chosen so that they were approximately equally detectable). Six sets of staircases were run. The results are as much like those of Figs 2 and 3 as the variability could possibly allow. Monocular viewing did not lead to any greater detectability of the compound gratings (relative to the simple ones) than did binocular viewing.

Other frequency pairs

We also collected some data for 6 c/deg paired with 3 c/deg and for 6 c/deg paired with 4 c/deg under the conditions described in Methods, including binocular viewing. Both observers viewed both of these frequency pairs in both the fovea and the periphery (7.5° to right) except that JGR did not view the 3 and 6 c/deg patterns in the fovea. In any one condition five sets of staircases were run. One phase ($\theta = 0$ in Eqn 3) was used. Five ratios of contrasts were used.

For 3 and 6 c/deg, the results looked as much like the results in Figs 2 and 3 for 2 and 6 c/deg as the variability could possibly allow. For 4 and 6 c/deg, the compound gratings may have been slightly more detectable relative to the simple gratings, particularly for the foveal condition. There was certainly no indication, however, of greater summation in the periphery than in the fovea.

Randomizing the position of the pattern

The observers intended to fixate steadily and believed they did, even when the stimuli were out in the periphery. The question naturally arises, however, as to whether they actually did so consistently.

The stimuli were brief (above 37% of peak amplitude for only 200 msec) in order to minimize the effect of saccades. The thresholds for the peripheral stimuli were a good deal higher than for the foveal (0.3 log units for 2 c/deg, and 0.5 log units for 6 c/deg), which means the observers' fixation was probably reasonably well maintained.

A corroborative result comes from some sessions in which the threshold for one frequency alone was measured at eight retinal positions randomly intermixed. As an observer could not know where the next stimulus was going to be, he should have been less tempted to move his fixation from the correct point. The thresholds measured in this condition, where the positions were randomly intermixed, were in no case more than 0.075 log units different from those measured in the main body of the experiments. This consistency suggests that in the main experiments also the observer was maintaining fixation. (Small differences between the results using randomly intermixed positions and those using a fixed position may be due to a position uncertainty effect analogous to the frequency uncertainty effect described in the next section.)

Frequency uncertainty effect

As the stimuli in this experiment, both simple and compound gratings, were randomly intermixed from trial to trial, the observer could never know which to expect. In the earlier study by Graham and Nachmias (1971), on the other hand, the stimuli were not intermixed. In that study, the compound gratings were found to be less detectable relative to the simple gratings than in the present study. That is, the points for the compound gratings were further from the origin (0,0) than those in Figs 2 and 3.

Such a difference is to be expected if there is a visual phenomenon analogous to the auditory frequency uncertainty effect (Green and Swets, 1966, section 10.4).

When the stimuli are randomly intermixed, the observer will probably attend equally to both frequencies (both channels). When the stimuli are not intermixed, however, the observer would be able to improve his performance in detecting the simple gratings (but not the compound ones) by attending to the appropriate frequency channel only. Such an improvement in simple grating performance would show up in plots like those of Figs 2 and 3 as a worsening of performance for compound gratings relative to simple gratings, i.e. as a displacement of the points for the compound gratings further from the origin (0,0). The points from Graham and Nachmias (1971) are indeed displaced in this way relative to the present study. Of course, there were many other differences between the two studies in addition to the intermixing of the stimuli (one of which is further discussed in the next section). Therefore, one cannot be certain that this was the factor responsible for the difference in results.

That the difference between not intermixing and randomly intermixing the patterns was probably the important difference between the two studies is suggested by a further brief experiment comparing blocks where the stimuli were intermixed with blocks where they were not. This experiment was run under conditions like those described in Nachmias and Weber

Table 1. The observed proportion correct from 600 trials for each of three patterns in two conditions and the proportion correct predicted from the probability summation model for the mixed f and $3f$ grating

Pattern	Mixed condition		Alone condition	
	Observed	Predicted	Observed	Predicted
f	0.70	—	0.77	—
	0.74	—	0.77	—
$3f$	0.69	—	0.79	—
	0.70	—	0.78	—
f and $3f$	0.80	0.82	0.81	0.90
	0.84	0.85	0.84	0.90

In each case two numbers are given, the top being observer SY's result and the bottom, observer CM's.

(1975). In particular, the gratings were centrally fixated; there was no spatial Gaussian weighting function; the onsets and offsets of the stimuli were sudden.

Three gratings were used—one of frequency 3 c/deg, one of 9 c/deg, and a compound of the two. For each of these three gratings, 600 trials were run in each of two conditions: intermixed (all three stimuli randomly intermixed) and alone (each stimulus presented many times in a row). A two-temporal alternative forced-choice procedure was used. Data were collected from two experienced observers who did not know the purpose of the experiment. Table 1 shows the results as proportion correct for the three patterns and also shows the predicted proportion correct for the compound grating using the simple multiple-channels probability summation model (see Eqns 4 and 5 in the next section). In the intermixed condition, the compound-grating results are consistent with the probability summation model. In the alone condition, however, the simple gratings are more detectable than in the intermixed condition, although the compound-grating detectability does not change. Thus, in the alone condition the compound grating is less detectable than predicted by the multiple-channels probability-summation model. In short, the results from the alone condition look like the earlier study, the results from the intermixed condition like those of the main experiment of the present study. The difference in Table 1 is small but probably large enough to explain the discrepancy between the two studies—a discrepancy which is small in terms of actual contrast values.

Extended uniform-contrast gratings

There is another possible cause of the difference between the results of the main experiment here (Figs 2 and 3) and those of Graham and Nachmias (1971). The stimuli in the present experiment were well localized patches of grating whereas the gratings of Graham and Nachmias were of uniform contrast extending over a larger portion of the visual field. However, with psychophysical procedures and conditions very similar to those used for the main experiment here (two-temporal-alternative, forced-choice, intermixed frequencies and contrasts, Gaussian time-course, same observers), Robson and Graham (in Graham, 1978) found that extended gratings behaved like the localized patches here. That is, the detectability of the compound gratings is consistent with the simple multiple-channels probability-summation model.[2] Thus, the difference between the results of Graham and Nachmias (1971) and those reported here cannot be simply attributed to grating extent, further supporting the view that the difference is due to a frequency uncertainty effect.

THEORY

The solid curves in Figs 2 and 3 are the predictions from a model in which there are multiple, independent channels sensitive to different ranges of spatial frequency. To describe this model and to contrast it with other, unsatisfactory, ones, several terms will be useful.

In a *single-channel model*, the important stage of the visual system is an array of overlapping receptive fields, all identical (e.g. of the same size). The positions of the receptive field centers are distributed uniformly across the visual field.

Each *receptive field* is assumed to be a linear system (that is, its response to the sum of any two inputs is the sum of its responses to each of the two inputs alone). Moderate departures from linearity, however, would make little difference to the predictions.

The model just described will sometimes be called a *space-invariant single-channel* model to distinguish it from a *space-variant single-channel model*. In the space-variant version (for example, Limb and Rubinstein, 1977), there is again a single array of receptive fields with only one receptive field centered at each point in the visual field. But the receptive fields are now not all identical but differ in size to allow for differences between fovea and periphery in spatial interaction characteristics.[3]

In a multiple-channels model, there are several superimposed arrays of receptive fields (i.e. several channels). All the receptive fields in a single array are identical, but those in different arrays differ in size and are thus sensitive to different ranges of spatial frequency. In particular, a channel sensitive to 2 c/deg is not sensitive to 6 c/deg and vice versa. In the space-invariant version of this model, each channel contains receptive fields throughout the visual field. Many space-variant versions could also be constructed to account for the differences at different eccentricities in the visual field. Since reasonable space-variant versions give rise to the same predictions for this experiment as does the space-invariant version, we will not distinguish here between space-variance and space-invariance in a multiple-channels model. However, it is quite possible that whether one does or does not assume space-invariance does make a difference for other classes of stimuli.

In short, a single-channel model postulates one receptive field at each position in the visual field with all receptive fields identical. A space-variant single-channel model postulates one receptive field at each position but the sizes of the receptive fields at different positions are different. A multiple-channels model postulates a number of sizes of receptive field at each position.

To predict psychophysical thresholds from these models, other properties must be specified. These properties and the models' predictions are described below. The derivations of the predictions are given in the Appendix.

[2] The results for extended gratings in Graham (1978) are plotted as psychometric functions. These results are well fitted by theoretical psychometric functions of the form of Eq 5 where the exponent has value 4.0 and probability summation among channels is assumed. Thus, as is explained in the Theory section, the amount of summation in these extended-grating results equals that shown by the outer of the two theoretical curves in Figs 2 and 3.

[3] The space-variant single-channel model might also be considered a multiple-channels model if one assumed that each channel contained only a limited number of receptive fields, all of identical size. Then the spatial regions of the visual field responded to by different channels would not overlap, and the model could be called "multiple channels at different positions". Here, however, the model will always be referred to as a "space-variant single channel".

A multiple-channels model

Suppose the channels are probabilistically independent. Then the probability of an observer *not* being correct on a given trial can be computed as the product of three probabilities: the probability that the channels sensitive to 2 c/deg do *not* detect the stimulus, the probability that the channels sensitive to 6 c/deg do *not* detect the stimulus, and the probability that the observer does *not* guess correctly. That is, letting P_c(stim) be the probability of an observer being correct, P_2(stim) and P_6(stim) the probabilities of the 2 and 6 c/deg channels, respectively, detecting the stimulus, and g be the probability of a correct guess (0.5 in this case):

$$1 - P_c(\text{stim}) = [1 - P_2(\text{stim})] \cdot [1 - P_6(\text{stim})] \cdot [1 - g]. \quad (4)$$

The assumption in Eqn 4 will be called the assumption of "probability summation among channels."

The model of detection implied by the guessing correction in Eqn 4 may well be wrong in detail, but no other model we have examined is completely satisfactory either. In any case, it does not appear that different detection models would lead to different conclusions about the present equation. We shall use the guessing correction in Eqn 4 because it has the advantage of being particularly convenient in conjunction with an analytical form to describe psychometric functions suggested by Quick (1974). According to Quick's suggestion, one can express the probability of a channel detecting a stimulus by the following simple equation:

$$P_i(\text{stim}) = 1 - 2^{-[c(\text{stim})S_i(\text{stim})]^k} \quad (5)$$

where S_i(stim) is the sensitivity of channel i to the stimulus, c(stim) is the contrast in the stimulus, and k is a parameter determining steepness of the function. As k approaches infinity, this function becomes steeper and steeper. If Eqn 5 holds with the same exponent for all channels, then it is easy to show that the psychophysical psychometric function will also have the form in Eqn 5. With an exponent near 3 or 4, this function is a good description of psychometric functions measured in the course of the present study.

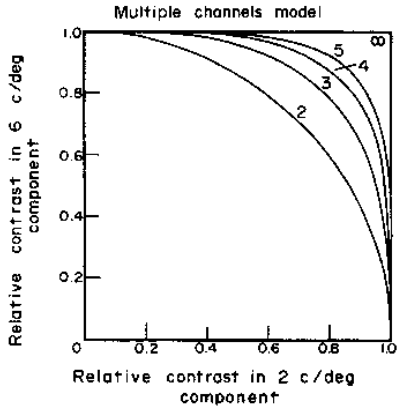

Fig. 4. Thresholds predicted by a multiple-channels model. Coordinates same as in Fig. 2. The different curves result from assuming psychometric functions of different steepness. See text for further details.

Equations 4 and 5 with the exponent k equal to 3 or 4 lead directly (e.g. Quick, Hamerly and Reichert, 1976; Appendix) to the predictions given by the solid curves in Figs 2 and 3 and shown again in Fig. 4 as the curves labelled 3 and 4. According to this model, the relative phase of the components should make no difference and thus each curve is a prediction for both phases. Curves for exponents in the range from 3 to 4 fit the data rather well.

If the exponent k is changed to two, however, the predicted summation curve (see Fig. 4) is one-fourth of the circle with radius 1. This curve is definitely too close to the origin to be consistent with the data. If k is changed to 5 or larger (Fig. 4), the predicted summation curve lies further away from the origin and is probably inconsistent with the data. The predictions for a k of ∞ are the upper and right edges of the square.

In a multiple-channels model, steepness of the psychometric function is not the only property which can cause the predicted summation curve to move toward and away from the origin in a plot like Fig. 4. Even if the steepness of the psychometric function is set at one value, the placement of the predicted curve will change if the degree of correlation between the variabilities in the two channels' responses is changed. The above predictions assumed probabilistic independence (Eqn 4). Suppose instead that the variabilities in both channels were perfectly positively correlated. Then, no matter what the steepness of the channel's psychometric function, the predicted summation curve would be the outside edges of the square because the same channel, whichever is most sensitive to the pattern, would detect the pattern on every trial. If the variabilities were negatively correlated, the predicted curves would lie closer to the origin than those predicted from independence. Summation experiments that only collect thresholds, therefore, like the experiments described here, are not ideal for deciding the detailed questions about variability in the channels.

However, the results of Sachs *et al.* (1971) give additional support to the assumption of complete independence among channels responding to frequencies as far apart as 2 and 6 c/deg. Further, values of k in the range from 3 to 4 do seem to fit psychometric functions extracted from the data collected in the staircases of the current experiment and also fit the psychometric functions collected separately by the method of constant stimuli.

At present, therefore, a reasonable summary of the data in Figs 2 and 3 is to describe it as consistent with a multiple-channels model in which the channels are probabilistically independent and their probabilities of response are described by an equation of the form suggested by Quick (Eqn 5) with a parameter k in the range from 3 to 4.

A single-channel model (space-invariant)

If a pattern is detected whenever at least one of the receptive fields in the single channel gives a large enough response, and if the variabilities in the responses of different receptive fields are perfectly positively correlated, then the predictions of the single-

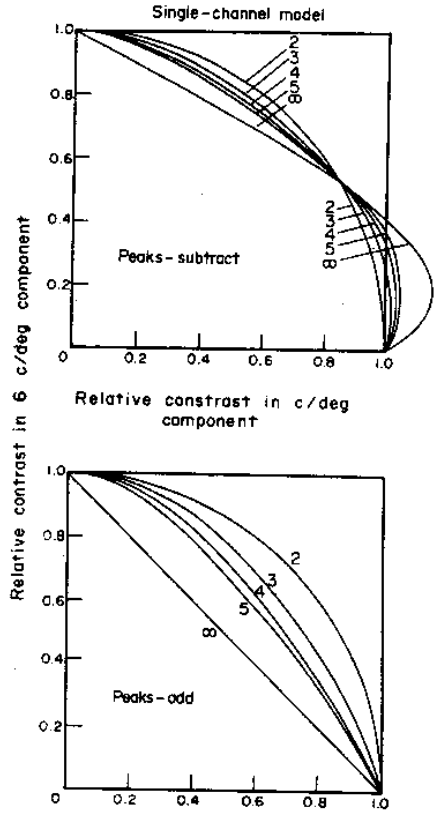

Fig. 5. Thresholds predicted by a model in which there is only a single channel (only one size of receptive field at each position in the visual field) and probability summation across space. Coordinates same as in Fig. 2. Predictions for peaks-subtract and peaks-add patterns are shown in the top and bottom panels, respectively. The different curves result from assuming psychometric functions of different steepnesses. See text for further details.

channel model for the experiment reported here are easy to derive (Graham and Nachmias, 1971) and are shown in Fig. 5 as the curve labeled ∞. For the peaks-add combination, there should be complete linear summation (the negative diagonal in the square); for the peaks-subtract combination there should be less summation but still a good deal. (The predictions are the same, both for extended sine-wave gratings and for the Gaussian-weighted patches of grating used in this study.) It is quite clear that none of our experimental results (Figs 2 and 3) are consistent with these predictions.

Probability summation across space. As Granger (personal communication) has pointed out, a relatively minor change in the assumptions of the single-channel model will make its predictions somewhat closer to the experimental results. Suppose that there is independent variability in the responses of receptive fields located at different positions. That is, suppose there is probability summation across space.[4] (Graham, 1978, attempts to give the intuition behind the results of making this assumption.) An easy way to deal quantitatively with this assumption is again to use Quick's suggested psychometric function (Eqn 5). This time the function is taken to describe the behavior of a single receptive field. Then the probability of detection is governed by an equation analogous to Eqn 4 since the variability in different fields is assumed independent. From these equations, it is easy to calculate the response of the single channel to any pattern (see Appendix). Figure 5 shows the predictions for the peaks-add and peaks-subtract gratings for various values of k. The predictions are the same both for extended sine-wave gratings and for the Gaussian-weighted patches of grating used in this study.

The predictions in Fig. 5 are not particularly sensitive to the form of the psychometric function. Granger (personal communication) and Limb and Rubinstein (1977) have used cumulative Gaussian psychometric functions and obtained very similar predictions.

None of the predictions in Fig. 5 describe the results in Figs 2 and 3. Thus a single-channel model, even including probability summation across space, cannot account for the results of sine-wave summation experiments.

It is worth noting that the predictions of a single-channel model with probability summation across space can sometimes be identical to those of a multiple-channels model with probability summation across different frequency channels (Quick *et al.*, 1976). The predictions for sine-wave summation experiments are identical when the variability (in the independent spatial positions or in the independent channels, respectively) is described by an exponent of 2.0 in Eqn 5 as can be seen in Figs 4 and 5. This is the case known in the auditory system as power summation. As Rashbass (1976) and Watson and Nachmias (1977) have pointed out, this case (applied to time rather than space) is also equivalent to Rashbass's (1970) model.

A single space-variant channel

What would a single space-variant channel predict for sine-wave summation experiments like those reported here? At first, one might suppose that the predictions would be like the multiple-channels predictions in Fig. 4 on the grounds that the 2 c/deg component might be detected by the larger receptive fields toward the peripheral side of the patch, and the 6 c/deg component by the smaller receptive fields toward the fovea. If the effect of eccentricity in the visual field was great enough, such a result would be predicted by the single space-variant channel model. However, calculations using the effect of eccentricity measured either with small patches of sinusoidal grating by us or with thin lines by Limb

[4] For a multiple-channels model, the possibility of probability summation across space is irrelevant for experiments, like this one, which use frequencies so far apart that no individual channel responds to both. For frequencies closer together, however, the question of probability summation across space within individual channels of a multiple-channel model is important. This question has been discussed by Stromeyer and Klein (1975), King-Smith and Kulikowski (1975), Graham and Rogowitz (1976), and Graham (1977, 1978).

and Rubinstein (1977) did not lead to this prediction. For patches of 2 and 6 c/deg sinusoidal gratings centered either at the fovea or 7.5° peripheral, the predictions looked just like the usual single-channel predictions (Fig. 5). This was approximately true for uniform sine-waves as well as for the gratings weighted by the Gaussian envelope used in this experiment (see Appendix).

Thus, the single space-variant channel models considered here, incorporating the effect of eccentricity measured by us or by Limb and Rubinstein (1977), cannot account for the sine-wave summation data in Figs 2 and 3.

CONCLUSION

The detectability of small patches of grating containing 2 c/deg, 6 c/deg, or both was measured in the periphery (7.5° to the right) as well as in the fovea. Within the precision of the experiment the results at the two positions were indistinguishable: a compound grating containing both 2 and 6 c/deg components was only slightly more detectable than the most detectable component by itself. Changing the phase of the components in the compound made no measureable difference. These results are consistent with a model postulating multiple independent channels, each sensitive to a different range of spatial frequency (Fig. 4). They are *not* consistent (Fig. 5) with a model containing only one size of receptive field at each position in the visual field (single-channel model), even if the receptive field size is assumed to vary in order to account for the differences in spatial interaction characteristic of different positions in the visual field (space-variant single-channel model).

Slight differences between some of these results and those of Graham and Nachmias (1971) may be due to a frequency-uncertainty effect.

REFERENCES

Aulhorn E. and Harms H. (1972) Visual Perimetry. *Handbook of Sensory Physiology*, Vol. VII/4. Springer–Verlag, Berlin.

Campbell F. W. and Green D. G. (1965) Optical and retinal factors affecting visual resolution. *J. Physiol., Lond.* **181**, 576–593.

Campbell F. W. and Robson J. G. (1964) Application of Fourier analysis to the modulation response of the eye. *J. opt. Soc. Am.* **54**, 581A.

Campbell F. W. and Robson J. G. (1968) Application of Fourier analysis to the visibility of gratings. *J. Physiol., Lond.* **197**, 551–566.

Doorn A. J. van, Koenderink J. J. and Bouman M. A. (1972) The influence of the retinal inhomogeneity on the perception of spatial patterns. *Kybernetik* **10**, 223–230.

Graham N. (1977) Visual detection of aperiodic spatial stimuli by probability summation among narrow band channels. *Vision Res.* **17**, 637–652.

Graham N. (1978) Spatial frequency channels in human vision: Detecting edges without edge detectors. In *Visual Coding and Adaptability* (edited by Harris C.). L. Erlbaum Assoc. Hillsdale, N.J.

Graham N. and Nachmias J. (1971) Detection of grating patterns containing two spatial frequencies: a comparison of single-channel and multiple-channels models. *Vision Res.* **11**, 251–259.

Graham N. and Rogowitz B. (1976) Spatial pooling properties deduced from the detectability of FM and quasi-AM gratings: a reanalysis. *Vision Res.* **16**, 1021–1026.

Granger E. (1973) An alternative model for grating detection. Paper presented at the meeting of the Association for Research in Vision and Ophthalmology, Sarasota, Florida, May, 1973.

Green D. G. (1970) Regional variations in the visual acuity for interference fringes on the retina. *J. Physiol., Lond.* **207**, 351–356.

Green D. M. and Swets J. A. (1966) *Signal Detection Theory and Psychophysics*. Wiley, New York.

Hilz R. and Cavonius C. R. (1974) Functional organization of the peripheral retina: sensitivity to periodic stimuli. *Vision Res.* **14**, 1333–1337.

Hines M. (1976) Line spread function variation near the fovea. *Vision Res.* **16**, 567–572.

King-Smith P. E. and Kulikowski J. J. (1975) The detection of gratings by independent activation of line detectors. *J. Physiol., Lond.* **247**, 237–271.

Kulikowski J. J. and King-Smith P. E. (1973) Spatial arrangement of line, edge, and grating detectors revealed by subthreshold summation. *Vision Res.* **13**, 1455–1478.

Lange R., Sigel C. and Stecher S. (1973) Adapted and unadapted spatial-frequency channels in human vision. *Vision Res.* **13**, 2139–2143.

Limb J. O. and Rubinstein C. B. (1977) A model of threshold vision incorporating inhomogeneity of the visual field. *Vision Res.* **17**, 571–584.

Mostafavi H. and Sakrison D. J. (1976) Structure and properties of a single channel in the human visual system. *Vision Res.* **16**, 957–968.

Nachmias J. and Weber A. (1975) Discrimination of simple and complex gratings. *Vision Res.* **15**, 217–224.

Pantle A. (1973) Visual effects of sinusoidal components of complex gratings: independent or additive? *Vision Res.* **13**, 2195–2204.

Quick R. F. (1974) A vector-magnitude model of contrast detection. *Kybernetik* **16**, 65–67.

Quick R. F. and Reichert T. A. (1975) Spatial-frequency selectivity in contrast detection. *Vision Res.* **15**, 637–643.

Quick R. F., Hamerly J. R. and Reichert T. A. (1976) The absence of a measurable "critical band" at low suprathreshold contrasts. *Vision Res.* **16**, 351–356.

Rashbass C. (1970) The visibility of transient changes of luminance. *J. Physiol., Lond.* **210**, 165–186.

Rashbass C. (1976) Unification of two contrasting models of the visual incremental threshold. *Vision Res.* **16**, 1281–1283.

Robson J. G. (1975) Regional variation of contrast sensitivity in the visual field. Paper given at the Association for Research in Vision and Ophthalmology, Sarasota, Florida, and unpublished observations.

Sachs M. B., Nachmias J. and Robson J. G. (1971) Spatial-frequency channels in human vision. *J. opt. Soc. Am.* **61**, 1176–1186.

Stromeyer C. F. and Klein S. (1975) Evidence against narrow-band spatial frequency channels in human vision: the detectability of frequency modulated gratings. *Vision Res.* **15**, 899–910.

Watson B. and Nachmias J. (1977) Patterns of temporal interaction in the detection of gratings. *Vision Res.* **17**, 893–902.

Wilson H. and Giese J. (1976) Threshold visibility of frequency gradient patterns. Paper given at the Association for Research in Vision and Opthalmology, Sarasota, Florida, and personal communication.

APPENDIX

The equations for the predictions shown in Figs 4 and 5 are derived here. Because the derivations for both sets of predictions involve some similar steps, we will start out using the neutral word "unit". In the multiple-channels

model, a unit will be an individual channel, namely, an array of receptive fields, all of the same size. In the single-channel model, a unit will be an individual receptive field at a particular spatial position.

Let P_i(stim) be the probability of the unit i detecting the stimulus. Let P(stim) be the probability of the observer detecting the stimulus. By assumption of completely independent units (that is, probability summation across channels or across spatial positions):

$$P(\text{stim}) = 1 - \prod_i [1 - P_i(\text{stim})]. \quad \text{(A1)}$$

This appendix will deal with P(stim). To relate this to 2-alternative forced-choice data, it is convenient to assume that P_c(stim), the probability of the observer being correct in a 2-alternative forced-choice situation, is related to P(stim) by

$$P_c(\text{stim}) = 1 - (1 - P(\text{stim})) \cdot (1 - g) \quad \text{(A2)}$$

where g is the probability of a correct guess—0.5 in this instance.

Under this assumption, there is a one-to-one relationship between P_c(stim) and P(stim). For example, P_c(stim) = 0.75 when P(stim) = 0.5. Thus it is sufficient to use a condition on P(stim).

Assume, as suggested by Quick (1974), that

$$P_i(\text{stim}) = 1 - 2^{-|R_i(\text{stim})|^k} \quad \text{(A3)}$$

where R_i(stim), the response of the unit, is linear with contrast. That is, if c is the contrast in the stimulus,

$$R_i(\text{stim}) = c \cdot S_i(\text{stim}). \quad \text{(A4)}$$

The quantity S_i(stim) is the constant of proportionality and equals the reciprocal of the threshold contrast for unit i. We are assuming here that threshold is that value producing a detection probability of 0.50 but, as is explained in the next section, any value could be assumed without changing the predictions.

It is easy to show, from Eqns A1, A3 and A4

$$P(\text{stim}) = 1 - 2^{-|R(\text{stim})|^k} = 1 - 2^{-|c \cdot S(\text{stim})|^k} \quad \text{(A5)}$$

where

$$S(\text{stim}) = \left\{\sum_i |S_i(\text{stim})|^k\right\}^{1/k} \quad \text{(A6)}$$

and

$$R(\text{stim}) = \left\{\sum_i |R_i(\text{stim})|^k\right\}^{1/k}. \quad \text{(A7)}$$

At psychophysical threshold (where P(stim) = 0.50), R(stim) = 1. Also, the reciprocal of the psychophysical contrast threshold is S(stim).

The stimulus used in these experiments will be denoted $(c_1 f_1, c_2 f_2)$ where c_1 is the contrast in the component of frequency f_1 and c_2 is the contrast in the component of frequency f_2. For simplicity's sake, phase is not explicitly represented in this notation and will be kept track of separately. The symbol $(c_1 f_1)$ will mean a grating containing only frequency f_1. $S_i(f_1)$ and $S(f_1)$ will give the sensitivities to frequencies f_1 of unit i and of the observer, respectively.

Notice that the quantities plotted in Figs 2, 3, 4 and 5 are: $x = c_1 S(f_1)$ for the horizontal coordinate, and $y = c_2 S(f_2)$ for the vertical coordinate.

Choice of threshold criterion

That P(stim) = 0.50 is taken as the threshold criterion is not limiting. Any other criterion would have led to the same predictions. An easy way to see this invariance with threshold criterion is to note that one could change the threshold criterion (e.g. to 0.25 instead of 0.50) just by changing the base in Eqn A3 from 2 to some other number (e.g. 1/0.25 = 4). Such a change leaves everything else untouched; for example, R_i(stim) still equals 1 at threshold. Thus the predictions remain the same.

The multiple-channels model

We will assume that there is no channel sensitive to both 2 and 6 c/deg. (Recall that, even considering the frequencies introduced by the Gaussian envelope, there is a wide separation between the 2 and 6 c/deg components.) There may be more than one channel sensitive to each alone, but we can group the channels sensitive to a given frequency together and refer to them as a single one without loss of generality. Thus, let channel number 1 (unit number 1) be the channel sensitive to 2 c/deg, and let channel number 2 be the channel sensitive to 6 c/deg. Since each channel only responds to one of the components in the compound gratings

$$\begin{aligned} R_1(c_1 f_1, c_2 f_2) &= R_1(c_1 f_1) = c_1 \cdot S_1(f_1) \\ S_1(f_1) &= S(f_1) \end{aligned} \quad \text{(A8)}$$

and similarly for frequency f_2. Then, by Eqns A7 and A8,

$$R(c_1 f_1, c_2 f_2) = \{|c_1 S(f_1)|^k + |c_2 S(f_2)|^k\}^{1/k}. \quad \text{(A9)}$$

At psychophysical threshold, therefore, where R(stim) = 1,

$$1 = \{x^k + y^k\}^{1/k} \quad \text{(A10)}$$

where x and y are the horizontal and vertical coordinates in Fig. 4.

The single-channel model (space-invariant)

Let unit i be the receptive field centered at position x_i. Since we are assuming these receptive fields are linear systems, it is easy to give the response of each unit to a pattern consisting only of two sinusoidal components (without a Gaussian envelope). Let a_1 and a_2 be constants expressing the relative sensitivity of each individual unit of the two frequencies f_1 and f_2. (The relative sensitivities are the same for all units since the units are from a single space-invariant channel.) Then the response of each unit to a compound grating will simply be the sum of its responses to the two components, that is, the response of the i^{th} unit will be

$$R_i(c_1 f_1, c_2 f_2) = c_1 a_1 \sin(2\pi f_1 x_i) + c_2 a_2 \sin(2\pi f_2 x_i + \theta). \quad \text{(A11)}$$

And, by Eqn A7

$$R(c_1 f_1, c_2 f_2) = \left\{\sum_i |c_1 a_1 \sin(2\pi f_1 x_i) + c_2 a_2 \sin(2\pi f_2 x_i + \theta)|^k\right\}^{1/k}. \quad \text{(A12)}$$

From this expression, one can numerically calculate the curves shown in Fig. 5 by varying c_1 and c_2.

When $k = 2$, Eqn A12 can be simplified further and an explicit expression for the prediction in Fig. 5 can be derived. To derive this expression, it will be useful to substitute integration over an integral number of periods for the summation in Eqn A12. Such a substitution assumes that the spatial locations x_i are numerous and spread out evenly, and that the summation occurs over a large spatial extent (or over an integral number of periods of the stimulus).

Also recall the following relations: for any two frequencies f_1 and f_2, integrating over an integral number of periods

$$\int (\sin 2\pi f_1 x)(\sin 2\pi f_2 x)\,dx = 0$$

and

$$\int \sin^2(2\pi f_1 x)\,dx = I$$

where I is a constant independent of frequency. Using the above, Eqn A12 becomes, no matter what the phase θ,

$$R(c_1f_1, c_2f_2) = [c_1^2a_1^2I + c_2^2a_2^2I]^{1/2}. \quad \text{(A13)}$$

At threshold, the value of the above expression is 1.0. Setting c_2 equal to zero shows that $S(f_1) = 1/c_1 = a_1I^{1/2}$. Similarly for $S(f_2)$. As can be seen by substituting $S(f_1)$ and $S(f_2)$ into Eqn A13, the prediction from this model at threshold is identical to that of the multiple channels model with $k = 2$ (Eqns A9 and A10). For both models the predicted curve is one-fourth of the unit circle.

Space-variance and patterns weighted by a Gaussian envelope

The derivations above assumed a space-invariant single-channel model and sinusoidal gratings uniform in amplitude across the visual field. It is quite easy to modify the derivation so that it takes space-variance into account and applies to gratings that are not uniform in amplitude.

To modify the derivations for space-variance, simply let a_{1i} and a_{2i} be the sensitivity of the receptive field at point i to frequencies f_1 and f_2. (The numerical values of a actually used are described below.) The response of the receptive field at point i to a combination of f_1 and f_2 will then be

$$R_i(c_1f_1, c_2f_2) = c_1a_{1i}\sin(2\pi f_1x_i) + c_2a_{2i}\sin(2\pi f_2x_i + \theta). \quad \text{(A14)}$$

To extend the derivations to apply to patterns that are not uniform in amplitude but, like the patterns used in this study, are weighted by a Gaussian envelope, is also simple. One multiplies R_i in Eqn A11 or A14 (for space-invariance or variance, respectively) by the Gaussian envelope and then applies Eqn A7. To do this is to ignore the frequencies other than 2 and 6 c/deg introduced into the pattern by the Gaussian envelope. However, since these frequencies are all very close to 2 and 6 c/deg, ignoring them should make little difference.

Predictions. Predictions were calculated for four conditions: for a model that was space-variant or space-invariant combined with patterns that were uniform in amplitude or weighted by a Gaussian envelope. (The patches of uniform-amplitude gratings were 4.5° in diameter and effects at the edge were ignored.[5] The Gaussian envelope was that of Eqn 2.) The predictions shown in Fig. 5 were introduced as being from a space-variant model combined with patterns uniform in amplitude. As it turns out, the predictions from all four conditions are very close. With one exception, the predictions from all four conditions are within 1.5% of each other. In the exceptional case, where k is infinity and the patterns of peaks-subtract phase, a space-variant model seems to lead to a predicted curve that is somewhat closer to the unit circle than is the curve shown in Fig. 5 predicted by a space-invariant model. (This apparent exception, however, may simply be an artifact of how close together the positions x_i used in the sum were. For a k of infinity, one needs very close positions to avoid missing the exact location of the maximum.)

Sensitivity as a function of eccentricity. In the experiments in which the sensitivity for patches of 2 and 6 c/deg alone were measured at several eccentricities, we found that sensitivity declined monotonically from the foveal center to 9° peripheral. The rate of decline was approximately 0.04 log units per degree for 2 c/deg and 0.065 log units per degree for 6 c/deg. Robson (1975), Hilz and Cavonius (1974), and Wilson and Giese (1976) found that, under their experimental conditions, sensitivity for all frequencies was maximal at foveal center.

Limb and Rubinstein (1977) used combinations of lines to estimate the sensitivity to different frequencies at different eccentricities. According to their measurements, sensitivity for 6 c/deg is almost constant for the first degree out from the foveal center and then declines. But sensitivity to 2 c/deg is not maximal at foveal center. It is actually maximal between 50 and 100 arc min away from the foveal center. It declines quite steeply toward the foveal center and somewhat less steeply toward the periphery. In the region near 7.5° peripheral, their measurements were very similar to ours.

In order to maximize any effect of space-invariance, a slightly more dramatic version of Limb and Rubenstein's foveal results was used to determine the values of a in Eqn A14 when making the predictions. The sensitivity to 6 c/deg was assumed to fall monotonically with distance away from foveal center at a rate of 0.0625 log units per degree. The sensitivity to 2 c/deg was assumed to increase monotonically from the foveal center to 1 degree away at a rate of 0.023 log units per degree and then to fall monotonically from that point outward at a rate of 0.06 log units per degree. As mentioned above, use of these values leads to predictions very close to those shown in Fig. 5.

Predictions were, in fact, also calculated using other, less dramatic, changes in sensitivity with eccentricity: those appropriate to the peripheral patches according to our measurements or the measurements of Limb and Rubinstein, and those appropriate to the foveal patches according to our measurements. As expected, these predictions were even closer to those for the space-invariant single-channel in Fig. 5.

[5] Limb and Rubinstein (1977 and personal communication) did not ignore effects at the edge, and these effects do make some difference. For example, in their calculations, the effects at the edge are responsible for the peaks-add combination of 3 and 9 c/deg being *less* detectable than the peaks-subtract combination for a grating of uniform contrast subtending 2.7°.